JJMIE

Volume 17, Number 2, June. 2023
ISSN 1995-6665
Pages 205– 218
https://doi.org/10.59038/jjmie/170205

Jordan Journal of Mechanical and Industrial Engineering

Thermal performance analysis of heat transfer in pipe by using metal foam

Raad Mohammed Kadhim Ali, Sajida Lafta Ghashim*

Mechanical Engineering Department, University of Baghdad, Baghdad, Iraq

Received 1 Feb 2023 *Accepted 23 Apr 2023*

Abstract

In this work, turbulent forced convection heat transfer in a circular horizontal pipe with insert of metal foam under the condition of constant heat flux is experimentally investigated. The Nusselt number (Nu) and friction factor (f) were tested under heat flux (31.8 and 42.4)KW/m^2 and water flow rates (3, 6 and 9) lit/min. Circular copper pipe with dimensions of 0.6 m in length, 0.025 m in diameter, and 0.001 m in thickness acts as the test section for the current investigation. It is heated by an electric heater mounted outside the pipe. The foam has pores per inch ranging from (10 to 40) PPI and porosity between (0.89 and 0.93).The water flowing through the pipe has a regular input temperature of 32°C.The temperature was measured along the pipe distributed in seven sections of the wall, in addition to measuring the temperature of entering and exiting the water from the pipe. The results show that, with a heat flux of 42.4 KW/m^2, the copper metal foam of 40 PPI gives a higher increase in average Nusselt number up to 73% as compared to metal foam of 10 PPI of 63.74%. The difference in pressure drop between pipes with and without metal foam varies just slightly at 10 PPI, but becomes greater at 40 PPI.

Keywords: Heat transfer coefficient, Pressure drop, Metal foam, Nusselt number, Porous media.

Nomenclature

A	area, m^2
C	inertial coefficient
Cp	specific heat capacity at a constant pressure , J/kg·K
f	friction factor
H	heat transfer coefficient, W/m^2.ºC
K	permeability of the metal foam, m^2
L	length of pipe , m
$\dot{m}$	mass flow rate, kg/s
Nu	Nuesslt number
P	pressure, Pa
Po	electrical power, W
PPI	pore per inch
Ø	rate of heat transfer, W
q″	heat flux per unit area , W/m^2
Re	Reynolds number
T	temperature, ºC
U	velocity, m/s
Vo	voltage, Volt
Z	axial coordinate, m

Greek symbols

μ	dynamic viscosity , kg/m·s
ρ	density, kg/m^3
λ	Thermal conductivity, W/m.ºC
β	permeability , m²
α	Permeability

Subscripts

bulk	bulk
cal	calculated
conv	convection
cond	conduction
i	inner
in	inlet
loss	total losses
o	without metal foam
s	surface
th	theoretical
wall	wall

1. Introduction

The strict requirements for heat exchange equipment improvement have led to the development of high-performance heat exchangers. The improvement of heat transfer in pipes has been the subject of numerous studies using a variety of methods, including twisted pipe Ray and Date [1] Yaningsih et al. [2] Bellos and Tzivanidis[3] and helical screw Sivashanmugam and Suresh [4] Sadeghi et al.[5].The effect of the twisted tape on heat transmission and pressure loss in a heat exchanger was investigated experimentally by Yadav [6]. The dimension of tank (0.8 m x 0.8 m x 1 m)and diameter of tube 5cm with length 1.85m.It depicts that, from results, the heat transfer coefficient increases by 40% with half-length twisted tape inserts when compared with plain heat exchanger. The

* Corresponding author e-mail: sajda_lafta@yahoo.com.

forced convection flow over two circular cylinders in a rectangular channel has been numerically simulated by Oyewola et al. [7].The Prandtl number (Pr) of air is 0.702 and the spacing ratios (S/D) are (1.1, 1.8, 2.0, 2.2, 2.4, 3.0, 4.0 and 5.0).The diameter of cylinder 0.1m,the length of the domain is 2D and the height is 4D. It is discovered that as S/D increases, the local Nusselt number on the four sections of the cylinders rises. Jawarneh et al. [8] conducts an experimental investigation on possible effects of jet vortex technology on the rate of heat transfer within a double pipe heat exchanger. The angle of inlet flow at four different levels 0°, 30°, 45°, and 60°. The Reynolds number was used for hot water in the annulus 10,000, 14,500, 18,030, and 19,600. The findings demonstrate that as the inlet flow angle and Reynolds number increases, the local Nusselt number and friction factor also increase. A porous material having a solid metal and either empty or fluid filled pores is called metal foam. Because natural metal foam contains structural and functional qualities, it is often employed in a different engineering use, like heat exchangers and electronic cooling, refrigeration and air conditioning, and aircraft. The metal foam distinct feature, which distinguishes him from traditional solid metal, has attracted a lot of attention and has potential application in a variety of industries such as vehicle body, grinding wheels and lubrication systems Nazirudeen and Dawood [9]. Inserting the high porosity metal foams is a successful passive technique that has generated a lot of interest Bose et al. [10]. An experimental and numerical model of heat transfer to study the impact the porosity of porous material by Heydaria et al. [11]. It is found from result the greatest porosity across the investigated porosity percentages for highest heat transfer for stable heat flux at the base is 36.6% for brass and aluminum fins and 31.6% for copper fin. The features of metal foam in terms of heat transmission and fluid flow have been carefully examined by experimental and numerical studies. Calmidi and Mahajan [12] used both mathematical and experimental approaches to examine the influence of inserting metal foam into a plexiglass tube and connecting it to a fan/motor system to create airflow within the tube. The governing equations are formulated in a quasi volume-averaged form for the numerical research. A variety of porosities and pore densities of aluminum metal foams have been used in experiments with air as the fluid medium. The upper side of the metal foam is provided with grooves, the heater is placed on the surface at a depth of 2 mm, and a surface-mounted thermocouple is inserted within. According to the results, the solid matrix's generally high conductivity reveals the transport-enhancing impact of thermal dispersion for foam-air combinations to be remarkably low. An Experimental model produced by Dukhan [13] aimed to study the pressure drop for flow inside an open loop tunnel. The size of tunnels was 14.5 cm by 30.2 cm. The thickness of test section was 5 cm. The porosity of the foam was (0.92 to 0.94) and the pore density (10,20 and 40) PPI. The findings show that when the velocity increases and foam porosity decreases, pressure drop increases. To explore the thermal efficiency of heat exchanger, Zhao et al. [14] developed an experimental and mathematical model. The heat exchanger is made up of two concentric pipes that form an inner and an outer annular section, both of which are embedded with metal foams. Both parts have axial, counterflowing fluid flow. It is considered that the outer pipe is completely insulated to ensure that there is no heat transmission between the pipe's outside surface area and its surroundings. In a tube heat exchanger, the influence of a metal-foam insert on heat transfer and fluid flow is investigated by varying the parameters of porous structure, permeability, physical size, etc. It is shown that an increase in pore density (PPI) or a decrease in porosity improves the efficiency of heat exchangers containing metal foam. A tube in tube heat exchanger investigated numerically by Du et al. [15], the solid-fluid conjugated heat transfer for the metal foam-filled double-pipe heat exchanger has been implemented using the two-equation model. The link between the inner and annular spaces was considered in the model. Specifically, it describes how certain factors affect the heat exchanger's performance and dimensionless excess temperature distributions. The two dimensions are assumed in this research, the results reveal that the heat transfer coefficient for the heat exchanger embedded with metal foam is much higher than smooth pipe. Also, heat transfer for the double pipe is enhanced with increase of the conductivity of metal foam due to increase of the fluid temperature and decrease of wall temperature which led to reduce thermal resistance. The heat transfer performance is enhanced with rises in the pore density and decrease of porosity because of the increase in the surface area of the foam and the diameter of cell ligament. Experimental research was done by Hutter et al. [16] to improve the pipe's ability to transport heat and to compare it to an empty pipe. The test section was metal foam embedded tubes, 200 mm in length, wound in a heating wire with a maximum power of 220 W, and coated in a fiber glass insulating sheet. The incompressible fluid, steady state, and homogeneity are assumed. The foam made of copper with (20 and 30) PPI has a mass flow rate range of (200 to 2500) ml/min. The findings show that metal foam has a five-fold greater capacity for heat transfer than an empty tube, and that this capacity increases with pore size. Xu et al. [17] used a channel of two parallel plates supplied with metal foam to examine the effects of local thermal non-equilibrium on the Nusselt number and pressure drop. The working fluid is air, and the heat flux applied to the plate is constant at 1000 W/m^2. The results demonstrate that the velocity increase near the wall with a foam-filled pipe that is significantly more than in a smooth pipe because the boundary layer is thinner. An experimental investigation conducted by Dukhan et al. [18] to study the effects of heat transfer in a cylindrical aluminum tube shows that an air-cooling system that includes metal foam desired half the pumping power of the water-cooling system while removing the same amount of heat and led to lowering the cost of producing air-cooled fuel cells. The tube has a 5.08cm diameter, 30.5 cm length, and 0.63 cm wall thickness. The metal's pore density is 20 PPI, and porosity 87.6%. The rate of heat flux is (15.518 and 26.865) W/m^2. The tube is covered with five layers of fiber ceramic due to insulate from ambient air. The results show that the wall temperature decreased with increase the flow velocity. The Nusselt number increase for local thermal non equilibrium of analytical solution compared with experimental solution and enhanced the heat transfer. Chen et al. [19] investigated numerically the influence Darcy number

(permeability) in a heat exchanger and the pipe was filled completely with metal foam and objected to variable heat flux. The results show that for filled pipe metal foam, the pressure drop rises with the decrease Darcy number because of increase resistance, the Nusselt number rises with increase the velocity fluid and decrease the Nusselt number higher 50 times more than the plain pipe. The total heat transfer of the doubled pipe heat exchanger increases with the decrease Darcy number and overall heat transfer coefficient rises with increase Reynolds number. A numerical investigated is presented by Xu et al.[20] to study the influence of properties of metal foam such as pore density and porosity on heat transfer performance. The radius of the tube is (0.001-0.05) m, porosity of metal foam is (0.80-0.97), pore density (3-70) and the Reynolds number (50-2000). The wall is subjected to constant wall temperature at 80 °C . The results reveal that the deference between the wall temperature and fluid temperature is decreased along the pipe due to rise the thermal conductivity. The local Nusselt number decreases with increase thermal conductivity ratio and it larger for LTE than LTNE due to increase in thermal resistance. An experimental study produced by Nima and Hajeej [21] aimed to investigate the influence of metal foam in a horizontal wined channel at different Darcy number and heat flux. The parameters of test section are: sides section (100 x 250 x 50) mm, length 500 mm and thickness 10 mm. The pore density of metal foam is (10 and 40) PPI and porosity (90.3, 89.9) %. Heat flux range (453, 1862, 3007, and 4462) W/m². Three heaters are putting in the bottom and top plate and covered with copper plate and the bottom side of the test section is protected by glass wool layer. The results indicated that the Nusselt number increases with decreasing Darcy number, and it was enhanced over 80% of the fluid case. Wang et al. [22] conducted an experimental study on the effects of heat transfer and flow resistance in a tube that had been filled with copper foam and nickel foam, respectively. The dimension of tube length 200mm and diameter 10mm. The pore density of metal foam 40 PPI . The tube was heated by resistance wire and insulator by aluminum silicate aspects with thickness 30mm and rapper pipe sleeve with 10mm thickness. The study indicated that the Nusselt number has risen as the Reynolds increases up, enhancing heat transmission. It was also discovered in this study that copper has superior heat transfer than nickel and smooth pipe due to copper's significantly higher thermal conductivity than nickel foam. The numerical research examines how the thermal performance of solar water collectors improved with insert metal foam done by Nima and Ali [23]. Solar collectors' type of flat plate provided with eight foam blocks was used. The conclusions indicate that the addition of metal foam blocks resulted in a decrease in the temperature of the absorber plate and a help in motivating in the heat transfer coefficient of more than 80%, which will lead to a rise in the temperature of the collector exhaust. A double pipe of heat exchanger is presented by Shi et al. [24] to study the effect of metal foam to enhance the heat transfer. The length of tube 1 m and the inner diameter 22 mm. The porosity of metal foam 0.9 and pore density (10,15 and 20) PPI. The water vapor is working fluid in this work. The metal foam is putting in outer pipe in the form of rings and the thermocouple is putting in the grooves on the surface of the tube. A new technique is presented by Anuar et al. [25] by using particle image velocimetry (PIV) and infrared thermography technique (IR) to inspect the impact of metal foam in a two different wined channel filled partially with different pore density (5, 10 and 30) PPI and various aspect ratio (0.05 to 0.39) of metal foam. An electric heater 3 kW are putting at the upstream of the test section. The predicted, it can see by PIV measurement was the velocity in the metal foam region is (1.6 and 1.8) times higher than the inlet velocity, the pressure gradient for 5 PPI metal foam is higher than (10 and 30) PPI of higher velocity. While the pressure gradient for 30 PPI metal foam is higher than 10 PPI for high aspect ratio. In order to study the effects of thermal conductivity and metal foam thickness on heat transfer, Kotresha and Nagarajan [26] used a vertical channel filled with various types of metal foam, such as copper 10 PPI and aluminum 10 PPI, with different thicknesses (10, 20 and 30) mm, and different the porosity of metal foam is used (0.85 and 0.95). The findings indicate that the pressure drop increased with greater mass flow rates and was larger for copper metal foam with a thickness of 30 mm compared to other materials. The Nusselt number increases as the thickness of the metal foam increases, and it is higher for copper metal foam than for aluminum metal foam because copper has a higher thermal conductivity. An experimental study produced Chen et al. [27] aimed to investigate the metal foam in a heat exchanger by placing 16 tubes (outer diameter 2mm and length 100 mm) embedded with metal foam in the form of circular rings in it. The parameter of the test section is (width =100mm, length =200mm, height =18mm), hot air is flowing in a rectangular channel (18 mm height and 100 mm width) that contained in the test section and it cooled by water. The pore density of metal foam is (20, 40, 60and 80) PPI and porosity (0.85 to 0.95). The findings indicate that the Nusselt number rises with increase porosity due to low flow resistance while the heat transfer rate rises with higher pore density and Reynolds number. Kotresha and Nagarajan [28]examined force convection heat transfer numerically in a channel that was partially filled with graded metal foam (20 and 40) PPI in a two-dimensional domain. The air entering the channel is moving at a rate of between (6 to 30)m/s, with the bottom wall estimated to have a constant wall temperature of 300 K. The data demonstrates that pressure drop and friction factor rise with an increasing input velocity while the pressure drop decreases for metal foam 20 PPI compared to 40PPI. The application of metal foam in the heat pipe radiator was examined by Shenming et al. [29] to develop heat transmission between the heat pipe and the air. Aluminum substrate, fins, and heat pipe are the three components of a heat pipe radiator. To increase the heat exchanger surface area, metal foam is applied to the fins. This study employs three different foam types (5, 15 and 25)PPI, with heat loads ranging from (5 to 25) W. The temperature of a heat pipe will always increase, but because of the metal foam's substantial surface area, the temperature of a metal foam heat pipe radiator (MFHPR) will always be lower than that of a pipe radiator without metal foam. To examine the cooling behavior of heat sinks constructed using PCM technology and combined with aluminum foam, the numerical model was presented by

AL-Migdady et al. [30].Three distinct values of the convective heat transfer coefficient (10, 20, and 30) W/m^2.K, two different PCM (RT35HC and RT44HC), and three different metal foam porosity (100%, 97%, and 90%) were used with a constant heat flux consumption of 3200 W/m^2. The dimension of rectangular enclosure is (46 mm × 30 mm). The results show that in comparison to the container with no metal foam, the basal temperature was reduced by (5 and 6) C^o by the RT35HC-based heat sink with aluminum foam inclusion of (0.97 and 0.90) porosity. Almonti et al. [31] the structure of foam was designed by CAD model. The pore density of metal foam are sample (4, 6 and 8)PPI and regular (4,6,8)PPI. The simple foam was tested experimentally by putting it in a sample holder and it exposed to air in a wind tunnel. The results show the thermal conductivity increased and enhancement for 8 PPI of metal foam due to increase the internal structure and turbulent flow developed easier. Numerical investigation presented by Jadhav et al. [32] was to study the effect of thermal performance and entropy generation by using Ansys fluent. The copper, aluminum and nickel metal foam filled partially in a tube. The metal foam at different pore density (10,20,30 and 40) PPI and porosities are (0.85 to 0.95). The Reynolds number at range from (1125 to 8500). The flow is assumed laminar, transition and turbulent. The results show that for laminar transition and turbulent flow regimes, the average wall temperature of copper foam is only 2.86%, 3.08%, and 2.85% lower than that of nickel metal foam for 40PPI with a porosity of 0.95; in contrast, the average wall temperature of aluminum for the same PPI is found to be closer to copper metal foam. Also, compared to nickel metallic foam and aluminum metal foam, copper metallic foam has a higher heat transfer enhancement ratio. Sabet et al. [33] used the Kelvin cell geometry for pore density 80 PPI and six different porosity by using Ansys Fluent program to study the nano porous model on heat transfer enhancement. The model is imposed to uniform heat flux. Gas rarefaction is very important in this research and is depended on the Knudsen Number (Kn). It can be observed from the result that the velocity is increment with increment the rarefaction for lower porosity. Due to decreased inertia forces (Darcy zone), the permeability increases with increasing Kn number and porosity. From the literature, despite the fact that there have been several experimental and numerical investigations on metal foams, the authors discovered that the influence of pore density and permeability has not been effectively addressed. The literature also lacks to adequately discuss the effects of the metal foam's height. Moreover, the authors discovered that metal foams were widely utilized for the goal of improving heat transfer, but that using it caused in a pressure loss. As a result, this research focuses on the experimental investigation of turbulent forced convection in the presence of open-cell metallic foam inside the pipe. The experiment is performed for two different PPI, specifically 10 PPI and 40 PPI, using various mass flow rate and heat flux parameters to achieve greater enhancement and acceptable pressure drop.

2. Experimental work

In Figure 1 and Figure 2, the experimental setup is depicted both photographically and diagrammatically. The following components comprise the test rig:

2.1. Test section

The test section is a circular copper pipe with a length of 0.6m, inner diameter of 0.025m and a wall thickness of 0.001m as indicated in the schematic Figure3a. An electrical heater was used to heat the surface of the outer tube, as depicted in Figure3b.The heater was wrapped around the pipe with equal distances between the coils to ensure uniform temperature distribution, the number of turns is 20 and the distance between the coils is approximately 2.5 cm. The heater is made of nickel-chrome wire that are 1 mm in diameter and are insulated by silica balls that are 0.05 m thickness. The maximum power in the wire was 2500 W. The voltage regulator provides AC current to the heater. An aluminum plate acts as the cover for the test section as shown in Figure 3c. To regulate the current in accordance with the desired heat flux, the circuit is coupled to a digital voltage regulator. The current flowing through the heater is measured using a digital clamp meter with a range of (0-200A) and accuracy of (±0.01A).

For the purpose of measuring the temperature on the surface of the test section, a small pipe with a diameter 0.003m and a length of 0.005m was welded, numbering six along the surface of the pipe, and the thermocouple was placed inside the pipe and fixed with silicone in order to give the best accurate reading. Also, two thermocouples were installed in the test section at the beginning and end of the pipe for the purpose of measuring the water temperature of the water. The maximum temperature range for K-type thermocouples (chromium – aluminum) is between (-200 and 1250) C$^\circ$. The sensor was made by joining the ends of the thermocouple wire, which was used to produce the temperature sensors. To fix the sensor and obtain a more stable reading, weld the thermocouple tip. The end of the thermocouple wire is connected to the digital thermometer (data logger) .Metal foam embedded pipe, two types of metal foam (10 and 40)PPI used in the present study as shown in Figure4.The metal foam sheet was cut into tubular sections using a water jet CNC machine ,it is carefully cut to a cylindrical shape to prevent damage to the metal foam's structure, and the outer diameter of the sample metal foam was specially designed to fit the inner diameter of the pipe and this it reduces the voids or gaps between the metal foam and surface of the pipe.

2.2. Heat exchanger

In the current experiment, a tube in tube heat exchanger made of copper was utilized. It comprises of an inner pipe placed concentrically inside a bigger pipe. The internal and external diameters are 0.016 m and 0.023 cm, respectively, with the length of the tube is 6m. The hot water flows in the external pipe while the cold water flows in the internal pipe in the counter direction, the heat exchanger is arranged in such configuration to meet the

different heat transfer requirements. The heat exchanger's purposes are to reduce the temperature of the water flowing out of the test section's outlet and to remove heat from the water.

2.3. Pump

The test section and the bypass pipe both get a portion of the water flowing through the circuit. The bypass pipe's function is to use a control valve to regulate the test section's water pressure and flow rate. To regulate the temperature of the water entering the test section, another line is utilized in the heat exchanger's circuit. Pump specifications: power of 0.37 kW, voltage of 220–240 volts, head of 7.27 m, discharge of 0.125 lit/min, maximum head of 40 m, and flow rate of 6.7 * 10^{-4} m^3/s lit/min were employed in the current work.

2.4. Tank supply

The centrifugal pump was placed at the same level as a 37-liter water tank that was 33x53x43 cm in size and 0.5 cm thick. The water tank was connected to the laboratory's water line's cold water inlet. Galvanized steel was used in the tank's construction.

2.5. Pipes and valves

To link the system's components, polyvinyl chloride (PVC) tubing with a diameter of 12.7 mm was used. The system has four valves.

3. Measurement tools

3.1. Electrical measurement

- The power source is connected to a voltage regulator (variance), which allows the user to alter the heater's power input rate as necessary. Digital voltmeters are parallel-connected to the circuit and the heating element to measure the voltage of the heater.
- The power of the heater is directly measured using a digital watt meter.
- A clamp meter is used to evaluate the current passing through the heater in order to confirm the measurements.

3.2. Temperature measurement

The temperature is measured using a digital thermometer (12 channels with memory card, model: BTM - 4208SD, Lutron Company, Taiwan).

3.3. Pressure management

A Borden gauge with a range of (0 – 1 bar) was used to estimate the pressure. These gauges are used to calculate the water's static pressure at the test section's inlet and exit. Pressure is also measured using a glass manometer with 2 m and 0.006 m dimensions.

3.4. Flow meter

Water flow meter of (0-20 lit/min) range with resolution 8.3*10^{-6} m^3/s.

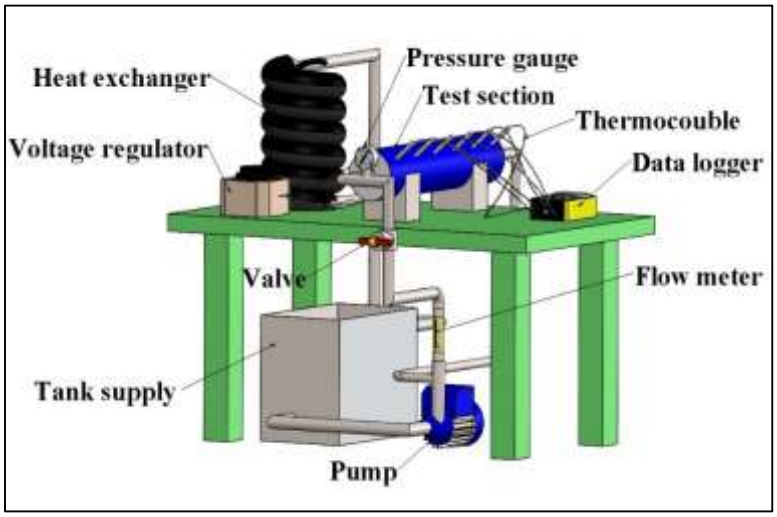

Figure 1..Photo of an experimental device designed using the SOLID WORKS software

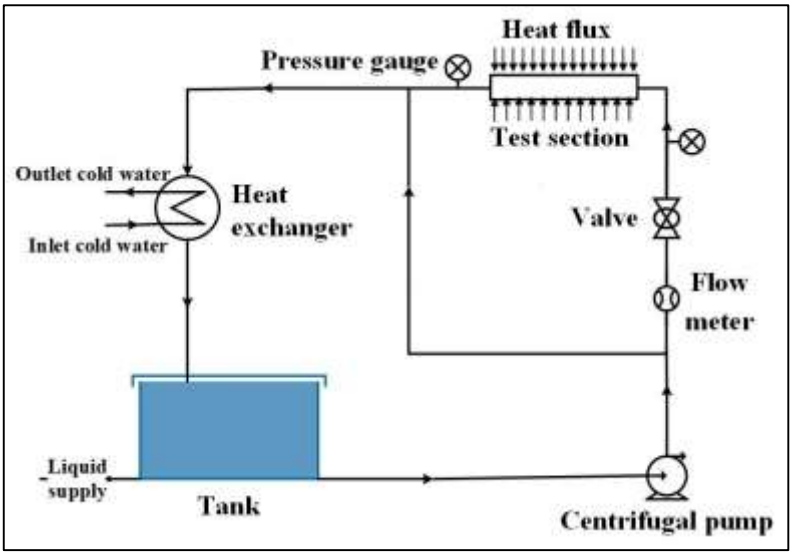

Figure 2. Diagram of experimental apparatus

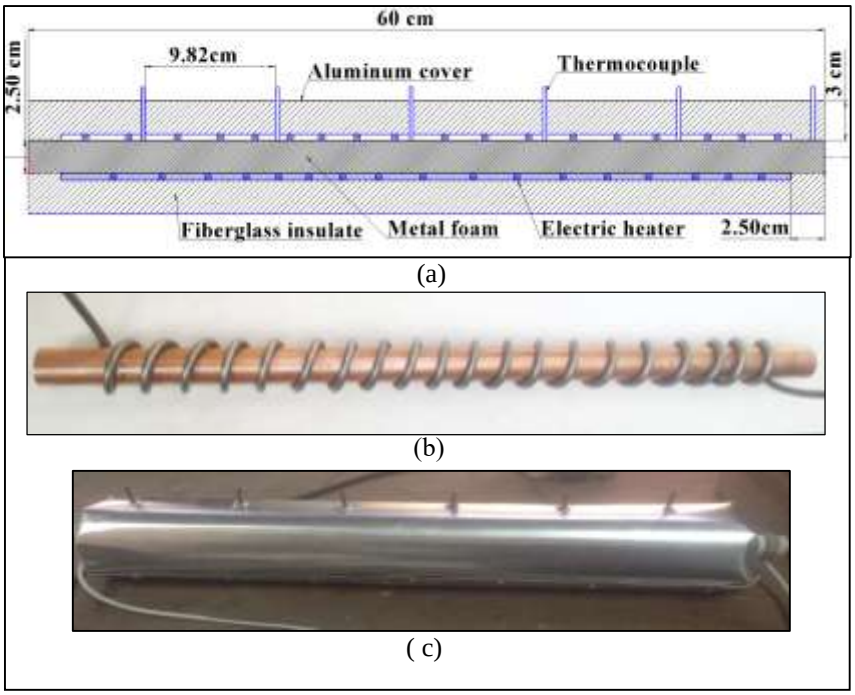

Figure 3. Schematic diagram of Test section

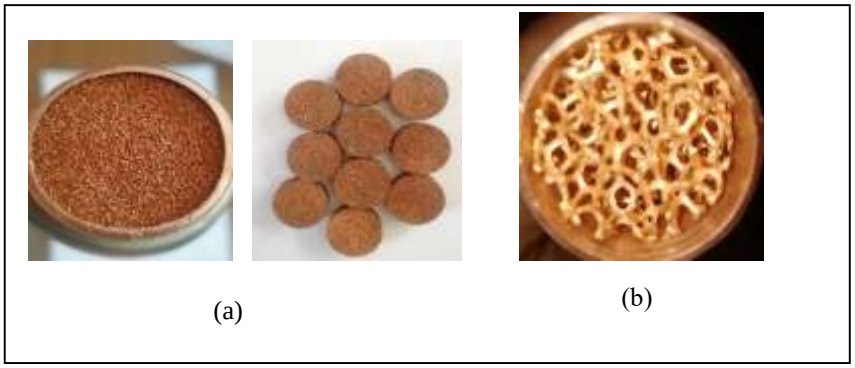

Figure 4. Photograph of test section and type of metal foam inside the pipe (a) 40 PPI (b) 10 PPI

4. Data reduction

The net heat flux is determined by Ezzat et al. [34], Ezzat and Ghashim [35]:

$$q" = \frac{\emptyset_{conv}}{A_s} \quad (1)$$

Where: $A_s = \pi \times D_i \times L$

The bulk temperature is calculating by:

$$T_{bulk}(z) = T_{in} + \frac{q" \pi D_i z}{\dot{m} cp} \quad (2)$$

The heater's electrical supply is determined by:

$$\mathrm{Po} = \mathrm{I}.\mathrm{Vo} \quad (3)$$

Where:

Po= electrical power

I= is the current flowing through the heater

Vo= is the voltage across the heater

The rate of heat transfer:

$$\emptyset_{conv} = Po - \emptyset_{loss} \quad (4)$$

Where:

$\emptyset_{loss}$is the sum of the radiation and conduction heat losses.

$$\emptyset_{loss} = \emptyset_{cond} + \emptyset_{rad} \quad (5)$$

$\emptyset_{radiation}$is very small, so it can be neglected.

$$\emptyset_{loss} = \frac{T_{wall} - T_{aluminum}}{\frac{ln\frac{r_2}{r_1}}{2\pi\lambda_{pipe}L} + \frac{ln\frac{r_3}{r_2}}{2\pi\lambda_{in.1}L} + \frac{ln\frac{r_4}{r_3}}{2\pi\lambda_{in.2}L} + \frac{ln\frac{r_5}{r_4}}{2\pi\lambda_{aluminum}L}} \quad (6)$$

The local heat transfer coefficient is presented in this equation Holman [36]:

$$h_z = \frac{q"}{(T_{wall(z)} - T_{bulk(z)})} \quad (7)$$

Average heat transfer coefficient:

$$h = \frac{1}{z}\int_0^z h_z \, dz \quad (8)$$

The following equation is used to determine the local Nusselt number:

$$Nu_z = \frac{h_z Di}{\lambda} \quad (9)$$

And average Nusselt number:

$$Nu = \frac{1}{z}\int_0^z Nu_z \, dz \quad (10)$$

The Reynolds number can be calculated using the inner diameter and fluid velocity at the entrance:

$$Re = \frac{\rho U D_i}{\mu} \quad (11)$$

The Nusselt number ratio is very important to evaluate the effect the heat transfer in the pipe and It defined as the ratio of the average Nusselt number of metallic foam pipe to plain pipe as shown in equation below:

$$\mathrm{Nu_{ratio}} = \frac{\text{Nu with metal foam}}{\text{Nu without metal foam}} \quad (12)$$

Based on exit the pressure difference between the tube's entrance and exhaust, the experimental fraction factor is computed using the following equation:

$$f = \frac{\Delta P}{\left(\frac{L}{D_i}\right)\left(\frac{\rho U^2}{2}\right)} \quad (13)$$

5. Parameters of metal foam

5.1. Porosity

Porosity (β) is a significant factor of metal foams and is dependent on both the size of the pores and the total volume of the sample containing the copper foams. The density and porosity of copper foams are:

$$\rho_{\mathrm{cal}} = \frac{\text{Mass}}{\text{Volume}} \quad (14)$$

$$\beta = 1 - \frac{\rho_{\mathrm{cal}}}{\rho_{\mathrm{th}}} * 100\% \quad (15)$$

Where

ρ_{cal}= calculated density of copper foams (required density).

Mass = weight of copper foams (kg) by using a digital sense scale(four digits).

Volume of the test section (m^3) = Length × Width × Height (by using adigital vernier scale).

ρ_{th}= theoretical density (copper 8933 kg/m^3) Incorpera et al. [37]

Experimental measurements revealed densities of 10PPI (866.301 kg/m^3) and 40PPI (909.575 kg/m^3). The porosity for the copper foams was (90.302%) for 10 PPI and (89.81%) for 40 PPI.

5.2. Permeability

Measurements of the pressure drop across the metal foam are done at various speeds and displayed to fit a second degree polynomial as specified by (Eq. 17). To determine the permeability and form drag coefficient, the equation is compared to the Darcy- Forchheimer relation Nield and Bejan [38] (Eq. 17). Figure 5 illustrates how pressure drop changes with Reynolds number. The inertial coefficient and permeability for each metal foam are listed in Table 1.

$$\frac{\Delta \mathrm{P}}{\mathrm{L}} = \mathrm{Au} + \mathrm{Bu}^2 \quad (16)$$

$$\frac{\Delta P}{L} = \underbrace{\frac{\mu}{\alpha}u}_{Darcy\ term} + \underbrace{\frac{\rho c}{\sqrt{\alpha}}u^2}_{\text{Forchheimer term}} \quad (17)$$

The formula for the permeability and form drag coefficient is:

$$\alpha = \frac{\mu}{\mathrm{A}} \quad (18)$$

$$C = \frac{\mathrm{B}\sqrt{\alpha}}{\rho} \quad (19)$$

Table 1. Properties of each metal foam

Pores per inch (PPI)	Permeability(α)	Inertial coefficient (C)	Porosity (β) %
10	7.859 x 10^{-8}	0.17	90.302
40	1.75 x 10^{-8}	0.159	89.81

6. Uncertainty analysis

Direct measurements were made of length, mass, time, and temperature. These numbers were uncertain due to mistakes made by the device manufacturers. The length, diameter, voltage and current had respective errors of ± (0.0005 m, 0.0005m, 0.01 V and 0.01A). The

thermocouple's inaccuracy in reading the temperature was ± (0.05) °C. Uncertainty analysis was used to evaluate the propagation of error in the derived quantities average flow velocity, Reynolds number, and Nusselt number. The suggested method of Holman [39], was used to evaluate the estimate of uncertainty associated with systematic error and random error. The uncertainty is given by:

$$\delta R = \frac{\partial R}{\partial x_1}\delta x_1 + \frac{\partial R}{\partial x_2}\delta x_2 + \cdots + \frac{\partial R}{\partial x_n}\delta x_n \quad (20)$$

$$W_R = \left[\left(\frac{\partial R}{\partial x_1}W_1\right)^2 + \left(\frac{\partial R}{\partial x_2}W_2\right)^2 + \cdots + \left(\frac{\partial R}{\partial x_n}W_n\right)^2\right]^{1/2} \quad (21)$$

Example

The Local Nusselt number depends on a number of variables, each subjected to uncertainty :

Nu= F (Vo, I, D_i, As, ΔT_x)

Where;

$\Delta T_x = T_{wall} - T_{bulk\ ave}$

The uncertainty can be given as follows;

$$W_{Nu} = \left[\left(\frac{\partial Nu_x}{\partial Vo}.W_{Vo}\right)^2 + \left(\frac{\partial Nu_x}{\partial I}.W_I\right)^2 + \left(\frac{\partial Nu_x}{\partial D_i}.W_{D_i}\right)^2 + \left(\frac{\partial Nu_x}{\partial As}.W_{As}\right)^2 + \left(\frac{\partial Nu_x}{\partial \Delta T_x}.W_{\Delta T_x}\right)^2\right]^{0.5} \quad (22)$$

Or,

$$\frac{W_{Nu}}{Nu} = \left[\left(\frac{W_{Vo}}{Vo}\right)^2 + \left(\frac{W_I}{I}\right)^2 + \left(\frac{W_{D_i}}{D_i}\right)^2 + \left(\frac{W_{As}}{As}\right)^2 + \left(\frac{W_{\Delta T_x}}{\Delta T_x}\right)^2\right]^{1/2} \quad (23)$$

The uncertainty of the friction factor, Reynolds number, and Nusselt number, respectively, is 12%, 14.12%, and 2.97%.

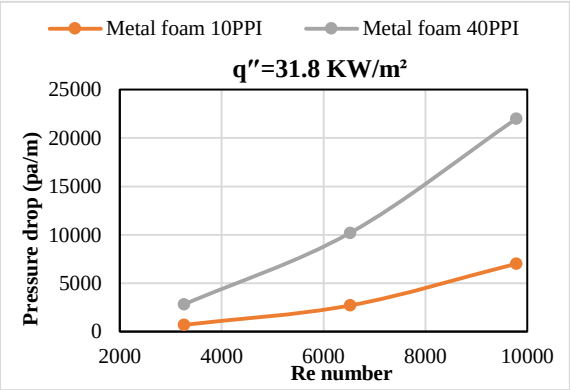

Figure 5. Pressure drop variation with Reynolds number

7. Verification of the results

The results are checked by using the correlation formulas of Nusselt number and friction factor for empty pipes using the V. Gnielinski equations Gnielinsk [40] , Cengel and Ghajar [41]and Blasius equation F. M. White [42], respectively. Figure 6 illustrates the relationship between average Nusselt number and Reynolds number and demonstrates acceptable accuracy, especially for high Reynolds number values, where the average error is less than 5%.For a heat flux of 31.8 KW/m^2, the friction factor of the current work and the friction factor calculated using the Blasius relation are compared in Figure 7. Values in the high Reynolds number chart demonstrate in clear that there is an acceptable degree of agreement between the data.

The Gnielinski formula is given by:

$$Nu = \frac{(f/8)(Re-1000)\,Pr}{1+12.7(f/8)^{0.5}(Pr^{2/3}-1)} \quad \text{For} \quad 10^3 < Re < 5\times10^6 \quad (24)$$

Where: $f = (1.58\ \ln Re\ 3.82)^{-2}$

The Blasius equation is given by:

$$f = 0.3164\,Re^{-0.25} \text{ For } 4\times10^3 < Re < 1\times10^5 \quad (25)$$

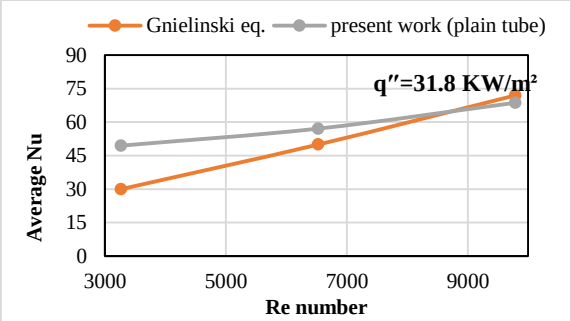

Figure 6. Comparison of the average Nusselt number with Gnielinski equation

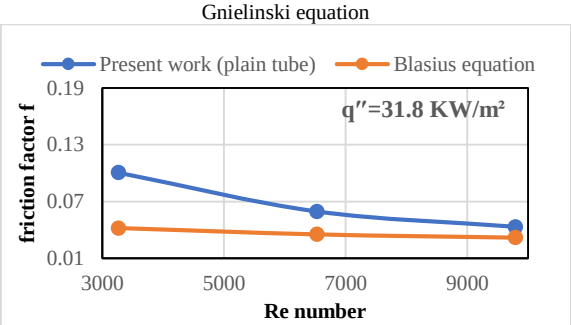

Figure 7. Comparison of the friction factor with Blasius equation

Additionally, in Figure 8 the experimental result for the average Nusselt number from the current study is validated using the numerical result from Jadhav et al. [32] for pore density 40PPI copper metallic foam. As can be seen from the figure, the discrepancy between the numerical and experimental results decreases as the mass flow rate increases since the air is used as the working fluid in the numerical research. Also, the first point of velocity used in numerical study is laminar, but the flow in the present research is turbulent. Nevertheless, from both the numerical and experimental results, the average Nusselt number rises as the Reynolds number rises.

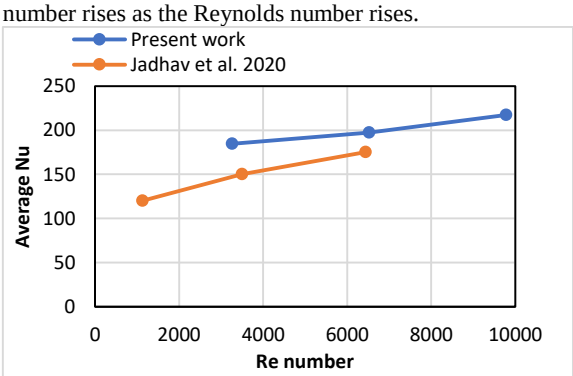

Figure 8. Comparison of the of average Nusselt number for 40 PPI

8. Results and discussions

The improvement of heat transfer in a pipe filled with metallic foam is examined in the experimental investigation. The pipe used for the experiments was designed to provide an uniform heat flux between (31.8 and 42.4)KW/m^2, and the flow's Reynolds number was between (3.2*10^3 to 9.7*10^3).

Figure 9 displays the wall temperature profile along the pipe at various water flow rates (3, 6, and 9) lit/min and range of heat fluxes (31.8 and 42.4) KW/m^2 for the case of empty pipe (without metal foam). It should be observed that each temperature curve's slope lowers as flow velocity rises. This indicates that the convection heat transfer from the heated wall is greater at higher velocities. Additionally, higher speed increases mixing and turbulence in the water flow, which improves the water's dispersion conductivity and improves surface conduction heat transfer. In addition, for the same Reynolds number value, the wall temperature rises as the heat flux increases because the buoyancy effect increases and accelerates the development of the thermal boundary layer along the pipe's surface. The distribution of the wall temperature for each type of metal foam (10 and 40) PPI is shown in Figure 10 and Figure 11as a function of applied heat flux variation and Reynolds number variation .It depicts that, an increase in Reynolds number results in a decrease in wall temperature at each metal foam. When the Reynolds number is raised, the heated wall's thermal boundary layer retreats at each metal foam. It is also discovered that, due to the additional surface area of the foam, the wall temperature decreased for metal foam embedded pipe with (10 or 40)PPI compared to empty pipes and decreased even more for pipes filled with foam 40 PPI at different heat flux.

Figures (12 to 14) demonstrate the bulk temperature variation along the pipe axis for several values of water flow rate (3, 6 and 9) lit/min and heat flux (31.8 and 42.4) KW/m^2.The figures show that that the distribution of temperature along the pipe rising linearly for any value of water flow rate and it reduces with increase the flow rate of water. Also, according to the figures, when there is a constant heat flux, the bulk temperature is influenced by the water flow rate, and the temperature decreases as the Reynolds number rises. In Figure 14 **,** the bulk temperature is increased sufficiently at 10 PPI in comparison to the empty pipe for any value of flow rate, and it rises at 40 PPI in comparison to 10 PPI because metal foam is present, which improves the fluid's thermal properties by increasing the surface area and, as a result, lowers temperature differences between the hot wall and the water.

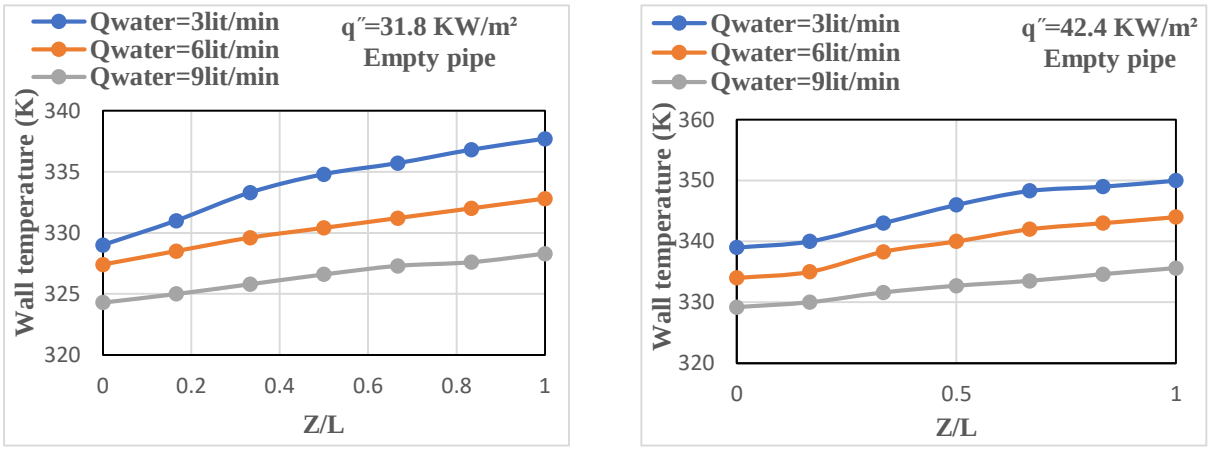

(a) (b)

Figure 9. Wall temperature variation along the pipe at different mass flow rate and heat flux

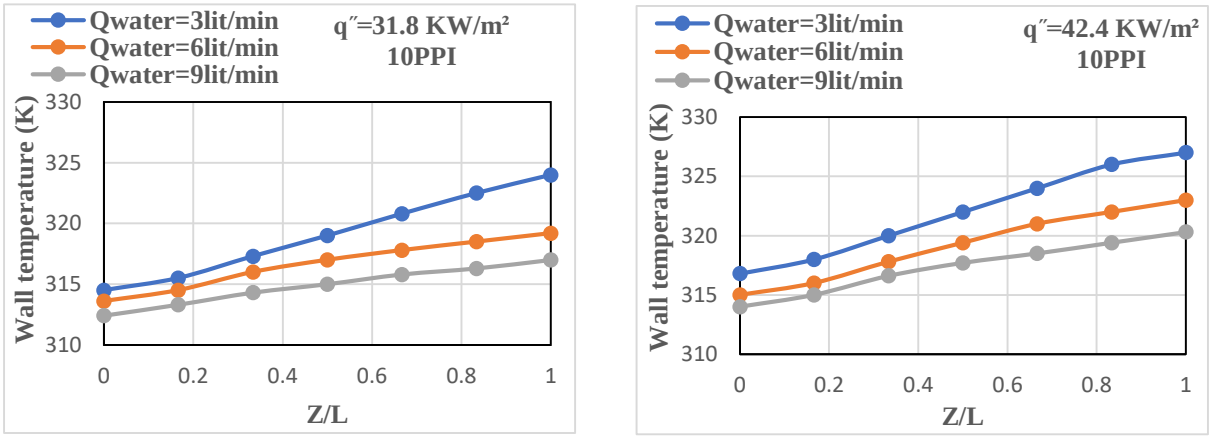

(a) (b)

Figure 10. Wall temperature variation along the pipe filled with metal foam 10 PPI

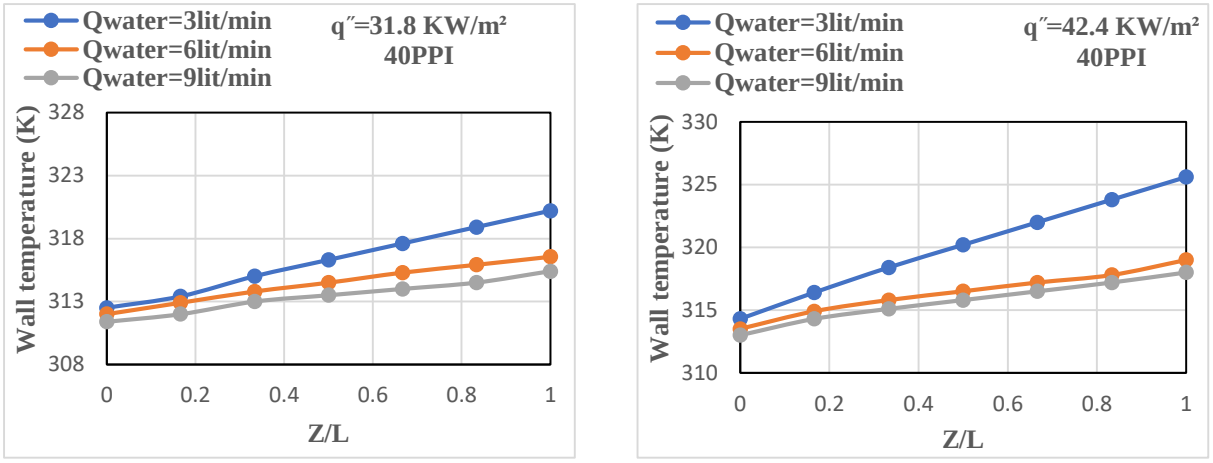

(a) (b)

Figure 11. Wall temperature variation along the pipe filled with metal foam 40 PPI

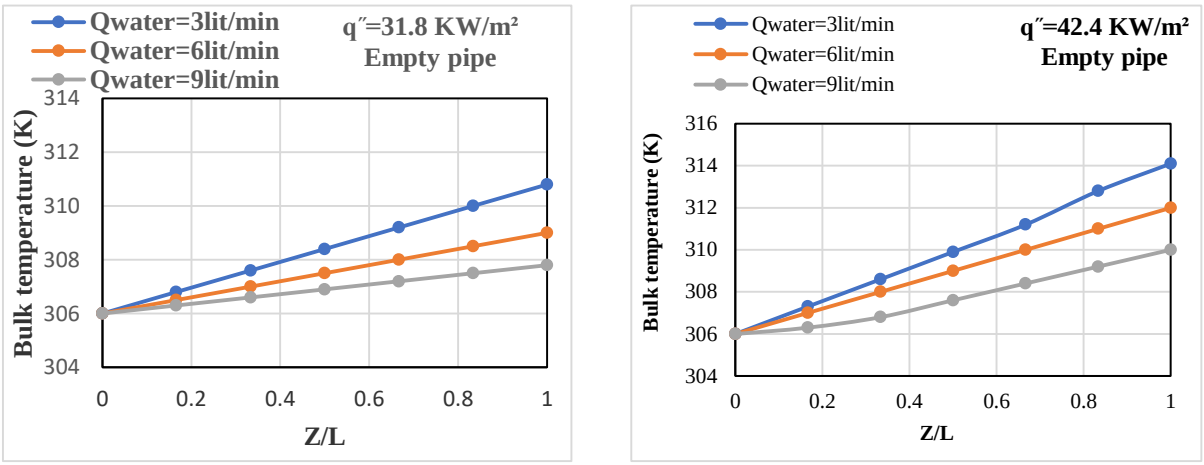

(a) (b)

Figure 12. Bulk temperature distribution along the pipe at different mass flow rate and heat flux

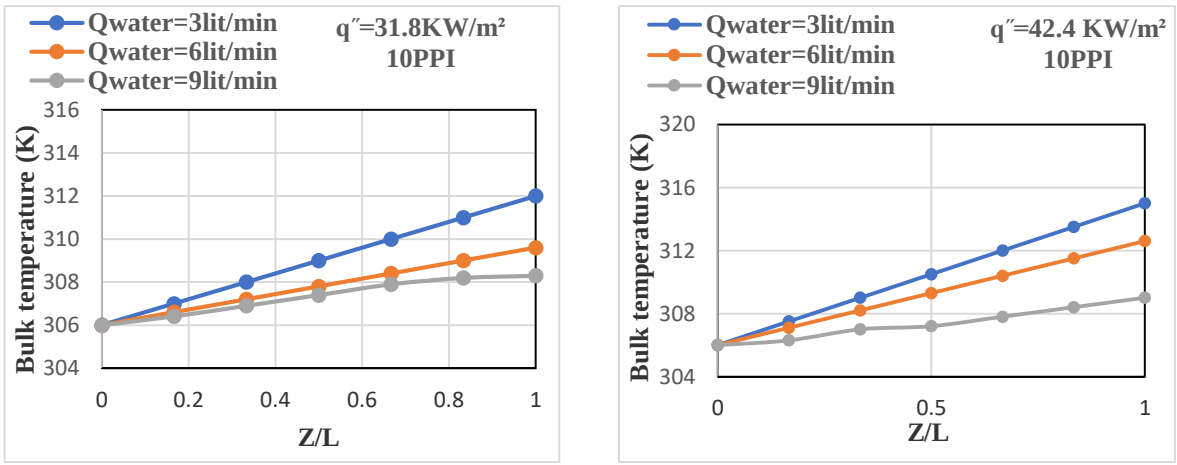

(a) (b)

Figure 13. Bulk temperature distribution along the pipe filled with metal foam 10 PPI

Figures (15 to 17) depict the variation of the local Nusselt number along a non-dimensional length of the pipe at various mass flow rates (3, 6 and 9) lit/min. The local Nusselt number always decreases as the axial distance rises for the pure pipe and the pipe with metal foam (10 and 40) PPI. Higher heat fluxes cause the buoyancy effect and the rate of thermal boundary layer formation to accelerate, which reduces the temperature differential between the heated surface temperature and fluid temperature along the pipe's axial distance. For the same Reynolds number value, it shows that the local Nusselt number rises as the heat flux rises. Additionally, it can be observed that the local Nusselt number in the case of the metal foam insert is significantly higher than that in the case of fluid (no metal foam) because the increased pore density of the foam increased the surface area of metal foam, which in turn increased heat absorption from the wall. The improvement in the local Nusselt number was 63.74% at 10 PPI and 73% at 40 PPI at higher heat fluxes 42.4 KW/m^2 and water mass flow rates 9 lit/min.

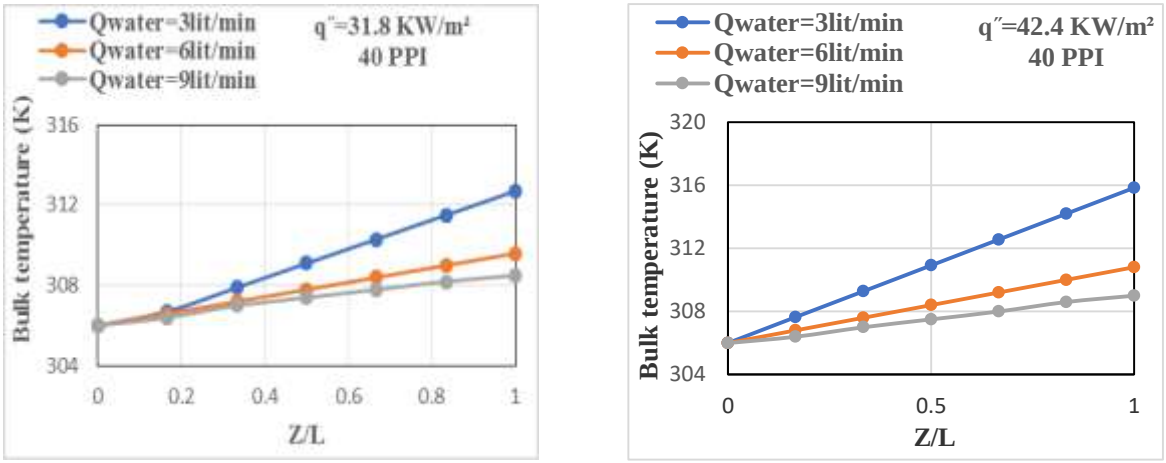

(a) (b)

Figure 14. Bulk temperature distribution along the pipe filled with metal foam 40 PPI

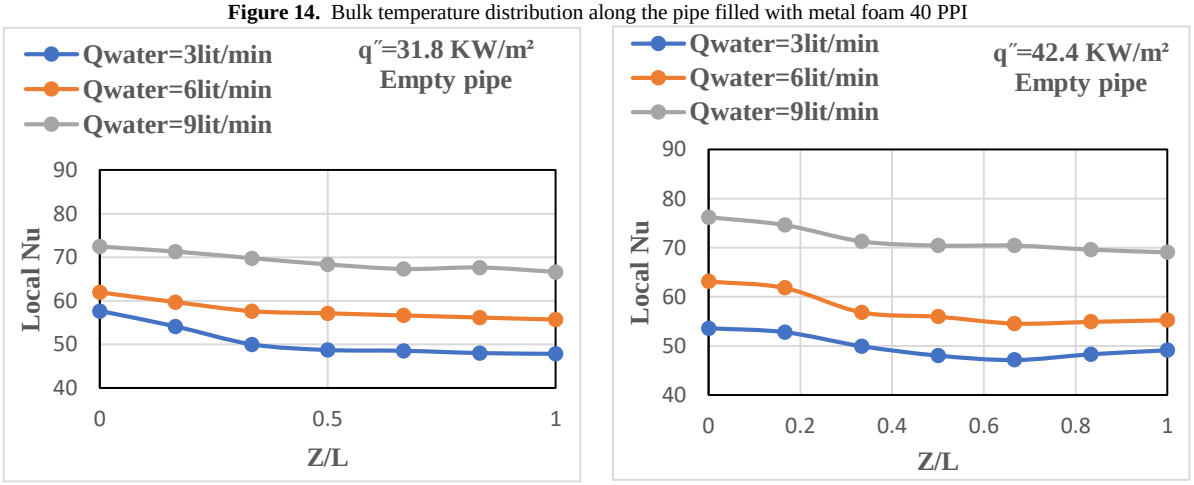

(a) (b)

Figure 15. Local Nusselt number distribution for the empty pipe at different mass flow rate and different heat flux

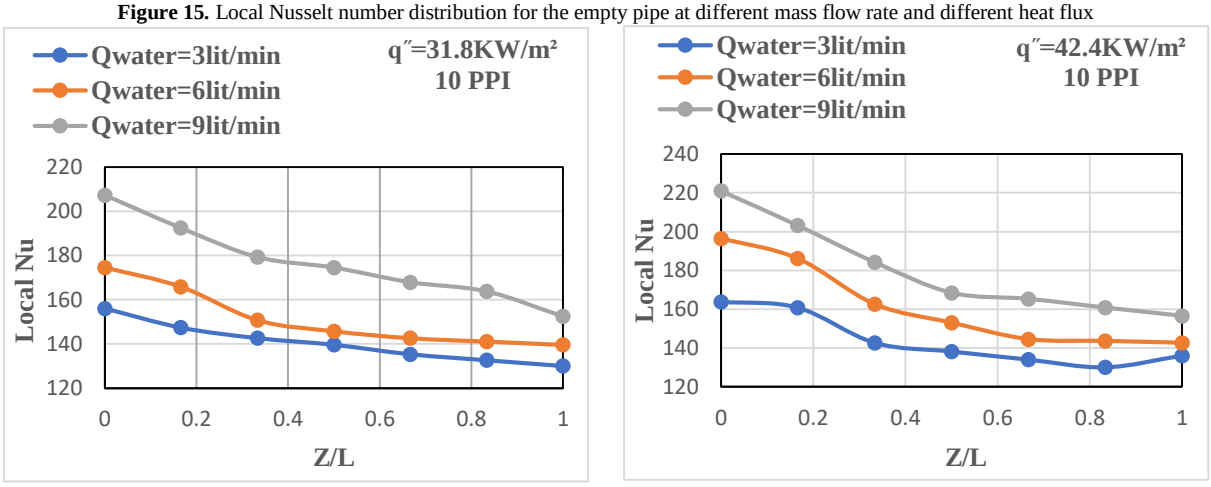

(a) (b)

Figure 16. Local Nusselt number of the pipe filled with metal foam 10 PPI

Figure 18 illustrates the distribution of the average Nusselt number as a function of Reynolds number for foamless pipe and with metal foam embedded pipe with (10 and 40) PPI at heat flux 31.8 KW/m^2. It demonstrates clearly that the average Nusselt number rises with increased Reynolds number for all pipe and that it is greater for pipe filled with 40 PPI of metallic foam because that foam is more highly conductive and it has a thinner boundary layer than foamless pipe. Figure19 illustrates how the pressure drop rises with rising Reynolds numbers and with the insertion of metal foam for two types (10 and 40) PPI. When metal foam is provided, the pressure drop significantly increases. Between the empty pipe and metal foam embedded pipe at high flow rates, there is a comparatively significant difference. As the water velocity is decreased, the divergence gradually gets smaller. However, the addition of metal foam, higher pore densities, or higher flow rates resulted in a greater pressure drop because more areas were in contact with each other, and increased the frictional resistance. In Figure 20, friction factor is given as a function of Reynolds number at constant heat flux 31.8 KW/m^2. Whereas foamless pipe's and 10 PPI metal foam specimen's friction factor are too close to each other, 40 PPI specimen has almost three times higher than 10 PPI sample

Figure 21 shows how metallic foam embedded in a pipe affects the Nusselt number ratio at a constant heat flux (31.8 KW/m^2).Two different kinds of PPI are used to measure the Nusselt number ratio along the pipe's length (10 and 40).It should be noticed that the Nu numbers obtained for the two models of foam display behavior that is quite similar, but with a high Nu number ratio for 40PPI metal foam. It is clear from the results of experiments that for obtaining a higher Nu number ratio higher pore specimens. Additionally, as the Reynolds number rises, the Nusselt number ratio decreases. So, a Nu number ratio for 40 PPI metallic foam is higher than the Nu number ratio of 10 PPI due to increase the surface area of metallic foam led to a rise in the thermal conductivity and enhancement in heat transfer.

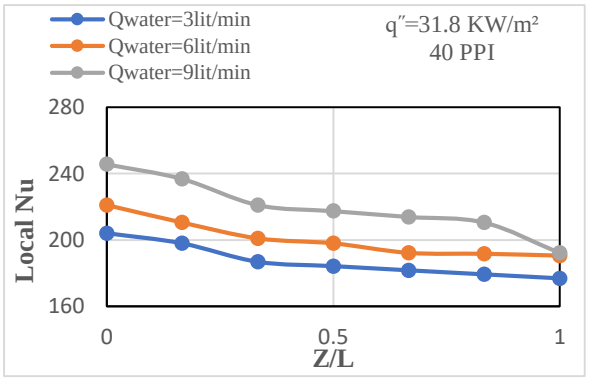

(a)

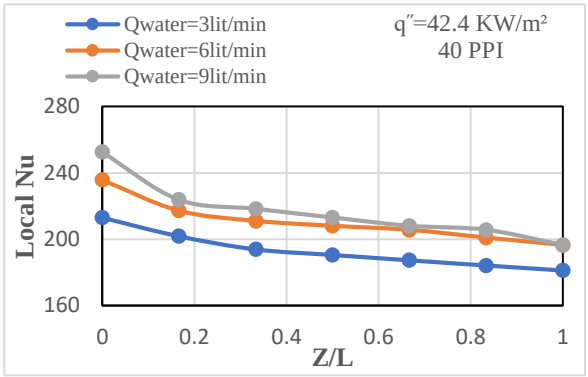

(b)

Figure 17. Local Nusselt number of the metal foam embedded pipe at 40 PPI

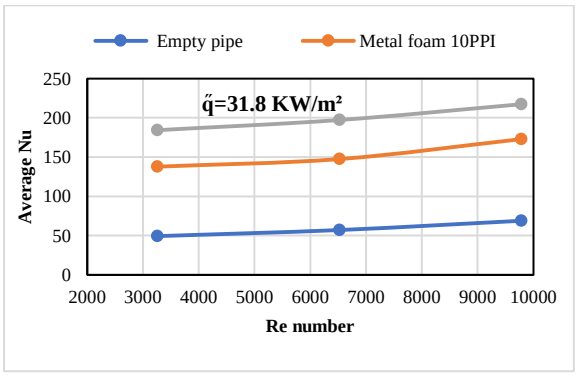

Figure 18. Variation of Average Nusselt number with Reynolds number

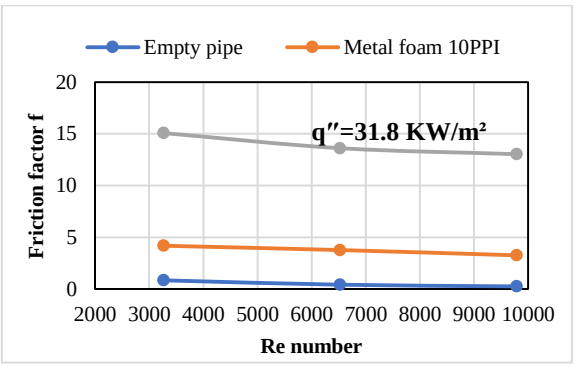

Figure 20. Variation of friction factor with Reynolds number

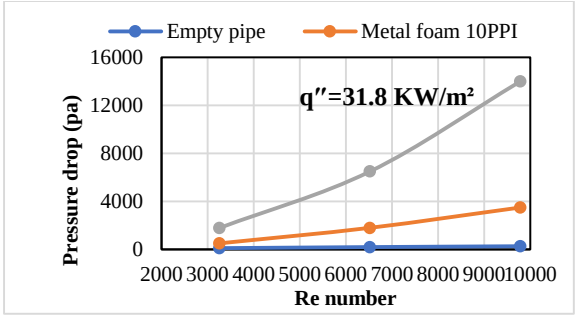

Figure 19. Variation of pressure drop with Reynolds number

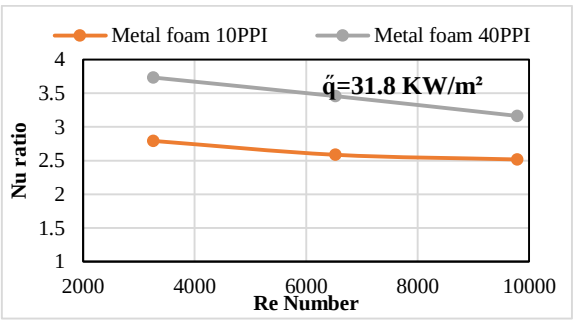

Figure 21. Variation of Nusselt number ratio with Reynolds number

9. Conclusion

In this work, an experimental analysis of the thermal influence of inserting metal foam into a pipe was suggested with the goal of enhancing thermal performance. The influence of two PPI on pressure drop and heat transfer were investigated. The heat fluxes (31.8 and 42.4) KW/m^2 and water flow rates (3, 6, and 9) lit/min were varied during the measurements. The following findings are reached:

1. The wall temperature increases in both cases with and without metal foam when the applied heat flux is increased. Also, the wall temperature decreases when metal foam embedded pipe because the metal foam's surface area and thermal conductivity are increased, which reduces thermal resistance and enhances heat transmission in the pipe.
2. The metal foam insert primarily enhances convective heat transmission because the presence of foam in the flow disturbs the thermal boundary layer and increases mixing of the flow.
3. For all input velocities, an increase in PPI causes an increase in pressure loss and thermal resistance. Metal foam embedded pipes have a higher pressure losses and frictional resistance factors than empty pipes.
4. The Nusselt number increases when Reynolds number and heat flux increases. The improvement in the Nusselt number was 63.74% at 10 PPI and 73% in 40PPI at higher heat flux 42.4 KW/m² and mass flow rate of water 9 lit/min.
5. The higher improvements in the Nusselt number ratio are indicated for the 40PPI copper foam pipe and the 10PPI foam tube are 20% and 13% when compared to the Nusselt ratio in the empty pipe at Re number 3.2*10^3 and heat flux 31.8 KW/m^2, respectively.

CRediT authorship contribution statement

The current concept was created by Sajida Lafta Ghashim. The testing and modeling were done by Raad Mohammed Kadhim Ali and Sajida Lafta Ghashim. The manuscript's final draft included contributions from Sajida Lafta Ghashim and Raad Mohammed Kadhim Ali. The project was supervised by Sajida Lafta Ghashim.

Conflict of interest

The authors declare that they have no conflict of interest.

References

[1] S. Ray and A. W. Date, “Friction and heat transfer characteristics of flow through square duct with twisted tape insert”. International Journal Heat Mass Transf., Vol. 46, No. 5, 2003, 889–902.

[2] I. Yaningsih, A. T. Wijayanta, T. Miyazaki, and and S. Koyama, “V-cut twisted tape insert effect on heat transfer enhancement of single phase turbulent flow heat exchanger”. AIP Conf.Proc., Vol. 1931, No. 1, 2018.

[3] E. Bellos and C. Tzivanidis, “Enhancing the performance of evacuated and non-evacuated parabolic trough collectors using twisted tape inserts, perforated plate inserts and internally finned absorber”. Energies, Vol. 11, May 2018.

[4] P. Sivashanmugam and S. Suresh, “Experimental studies on heat transfer and friction factor characteristics of turbulent flow through a circular tube fitted with regularly spaced helical screw-tape inserts”. Applied Thermal Engineering, Vol. 27, No. 8, 2007,1311–1319.

[5] O. Sadeghi, H. A. Mohammed, M. Bakhtiari-Nejad, and M. A. Wahid, “Heat transfer and nanofluid flow characteristics through a circular tube fitted with helical tape inserts”. International Commun. Heat Mass Transfer, Vol. 71, 2016 , 234–244.

[6] A. S. Yadav, “Effect of halflength twisted-tape turbulators on heat transfer and pressure drop characteristics inside a double pipe U-bend heat exchanger anil”. Jordan Journal of Mechanical and Industrial Engineering, Vol. 3, No. 1, 2009,17–22.

[7] O. M. Oyewola, O. S. Ismail, and K. Abu, “Numerical simulation of forced convection flows over a pair of circular cylinders in tandem arrangement”. Jordan Journal of Mechanical and Industrial Engineering, Vol. 13, No. 4, 2019, 221–230.

[8] A.M.Jawarneh, M. Al-Widyan and Z.Al-Mashhadani, “Experimental study on heat transfer augmentation in a double pipe heat exchanger utilizing jet vortex flow”. Heat Transfer, Vol. 52, 2022, 317- 332.

[9] S. S. M. Nazirudeen and A. K. S. Dawood, “A development of technology for making porous metal foams castings”. Jordan Journal of Mechanical and Industrial Engineering, Vol. 4, No. 2 , 2010, 292–299.

[10] J. R. Bose, S. Manova, L. G. Asirvatham, and S. Wongwises, “Comprehensive case study on heat transfer enhancement using micro pore metal foams: From solar collectors to thermo electric generator applications”. Case Study Thermal Engneering, Vol. 27, 2021.

[11] A. Heydaria, M. Mesgarpourb, and M. R. Gharib, “Experimental and numerical study of heat transfer and tensile strength of engineered porous fins to estimate the best porosity”. Jordan Journal of Mechanical and Industrial Engineering, Vol. 14, No. 3, 2020, 339–348.

[12] V. Calmidi and R. Mahajan, “Forced convection in high porosity metal foams”. Journal of Heat Transfer, Vol. 122, Aug. 2000.

[13] N. Dukhan, “Correlations for the pressure drop for flow through metal foam”. Experiment Fluids, Vol. 41, No. 4, 2006, 665–672.

[14] C. Y. Zhao, W. Lu, and S. A. Tassou, “Thermal analysis on metal-foam filled heat exchangers. Part II: Tube heat exchangers,” International Journal Heat Mass Transfer, Vol. 49, No. 15–16, Jul. 2006, 2762–2770.

[15] Y. P. Du, Z. G. Qu, C. Y. Zhao, and W. Q. Tao, “Numerical study of conjugated heat transfer in metal foam filled double-pipe”. International Journal Heat Mass Transfer, Vol. 53, No. 21, , 2010, 4899–4907.

[16] C. Hutter, D. Büchi, V. Zuber, and P. Rudolf von Rohr, “Heat transfer in metal foams and designed porous media”. Chemical Engineering Science, Vol. 66, No. 17, 2011, 3806–3814.

[17] H. J. Xu, Z. G. Qu, and W. Q. Tao, “Thermal transport analysis in parallel-plate channel filled with open-celled metallic foams”. International Communications in Heat and Mass Transfer, Vol. 38, No. 7, Aug. 2011, 868–873.

[18] N. Dukhan, Ö. B. ˘cı, and M. Özdemir, “Thermal development in open-cell metal foam: An experiment with constant wall heat flux”. International Journal Heat Mass Transfer, Vol. 85, 2015, 852–859.

[19] X. Chen, F. Tavakkoli, and K. Vafai, “Analysis and characterization of metal foam-filled double-pipe heat exchangers”. Numerical Heat Transfer, Part A: Applications, Vol. 68, Oct. 2015.

[20] H. J. Xu, L. Gong, C. Y. Zhao, Y. H. Yang, and Z. G. Xu, "Analytical considerations of local thermal non-equilibrium conditions for thermal transport in metal foams". International JournalThermal Science, Vol. 95, 2015, 73–87.

[21] M. A. Nima and A. H. Hajeej, "Experimental investigation of convection heat transfer enhancement in horizontal channel provided with metal foam blocks". Journal of Engineering, Vol. 22, No. 5, 2016,144–161.

[22] G. Wang, C. Qi, Y. Pan, and C. Li, "Experimental study on heat transfer and flow characteristics of two kinds of porous metal foam tubes filled with water". Thermal Science, Vol. 22, Jan. 2017.

[23] M. A. Nima and A. M. Ali, "Numerical study of heat transfer enhancement for a flat plate solar collector by adding metal foam blocks," Journal of Engineering, 2017, 13–32.

[24] J. Shi, G. Zheng, and Z. Chen, "Experimental investigation on flow condensation in horizontal tubes filled with annular metal foam". International Journal Heat Mass Transfer, Vol. 116, 2018, 920–930.

[25] F. Shikh Anuar, I. Ashtiani Abdi, and K. Hooman, "Flow visualization study of partially filled channel with aluminium foam block". International Journal Heat Mass Transfer, Vol. 127, 2018, 1197–1211.

[26] B. Kotresha and G. Nagarajan, "Effect of thickness and thermal conductivity of metal foams filled in a vertical channel – A numerical study". International Journal Numerical Methods Heat Fluid Flow, Jan. 2018.

[27] K. Chen, L. Guo, X. Xie, and W. Liu, "Experimental investigation on enhanced thermal performance of staggered tube bundles wrapped with metallic foam". International Journal Heat Mass Transfer, Vol. 122, 2018, 459–468.

[28] B. Kotresha and G. Nagarajan, "Analysis of forced convection heat transfer through graded PPI metal foams: Select Proceedings of NHTFF 2018". Lecture Notes in Mechanical Engineering, 2019, 151–158.

[29] X. Shenming, Y. Ran, S. Limei, W. Yupeng, X. Junlong, and C. huanxin, "The experimental study of a novel metal foam heat pipe radiator". Energy Procedia, vol. 158, 2019, 5439–5444.

[30] A. K. AL-Migdady, A. M. Jawarneh, A. K. Ababneh, and H. N. Dalgamoni, "Numerical investigation of the cooling performance of PCM-based heat sinks integrated with metal foam insertion," Jordan Journal of Mechanical and Industrial Engineering, Vol. 15, No. 2, 2021, 191–197.

[31] D. Almonti, G. Baiocco, E. Mingione, and N. Ucciardello, "Evaluation of the effects of the metal foams geometrical features on thermal and fluid-dynamical behavior in forced convection". International Journal of Advanced Manufacturing Technology, Vol. 111, No. 3–4, 2020, 1157–1172.

[32] P. H. Jadhav, G. Nagarajan, and D. A. Perumal, "Conjugate heat transfer study comprising the effect of thermal conductivity and irreversibility in a pipe filled with metallic foams". Heat and Mass Transfer, Vol. 57, No. 6, 2020, 911–930.

[33] S. Sabet, M. Barisik, B. Buonomo, and O. Manca, "Thermal and hydrodynamic behavior of forced convection gaseous slip flow in a Kelvin cell metal foam". International Communications in Heat and Mass Transfer, Vol. 131, 2022.

[34] A. Ezzat, N. Abdullah, and S. L. Ghashim, "Effect of air bubbles on heat transfer coefficient in turbulent convection flow". Journal of Engineering, Vol. 23, No. 1, 2017, 1–21.

[35] A. W. Ezzat and S. L. Ghashim, "Investigation of optimum heat flux profile based on the boiling safety factor". Journal of Engineering, Vol. 25, No. 4, 2019.

[36] J. P. Holman. Heat Transfer. Sixth Edition. McGraw-Hil; 1986.

[37] F. P. Incorpera, D. P. DeWitt, T. L. Bergman, and A. S. Lavin. Fundamentals of heat and mass transfer. 6th Edition.John Wiley, New York; 2006.

[38] D. A. Nield and A. Bejan. Convection in porous media. New York; 2006.

[39] J. P. Holman. Experimental methods for engineers. Eight Ed.McGraw-Hill Series in Mechanical Engineering; 2007.

[40] V. Gnielinsk, "New equations for heat and mass transfer in turbulent pipe and channel flow". International Chemical Engineering, Vol. 16, 1976, 359–368.

[41] Y. A. Cengel and A. J. Ghajar. Chapter 8 : Internal forced convection. 4th ed., New York McGraw Hilll; 2011.

[42] F. M. White. Fluid mechanics. 7th ed.. New York :McGraw-Hill; 2011.